6. Numerical Analyses of the Failure Processes of Foundation Piles and Buried Pipe during Earthquakes

In this chapter, the failure processes of RC piles and steel gas pipe damaged by the 1964 Niigata and 1983 Nihonkai-Chubu earthquakes, respectively, are investigated by numerical analyses. Based on these analyses, the vertical distributions of the permanent ground displacements, the friction strength between the liquefied soil and the pipes are also discussed.

6.1 Numerical analyses of RC piles damaged by the 1964 Niigata earthquake

As mentioned in Section 3.2, most of the reinforced concrete piles in the building near Niigata Station were found to have been completely broken at two elevations, as shown in Figure 3-10. Generally, two causes can be considered for this damage to the piles : liquefaction induced permanent ground displacements and excessive inertia forces from the superstructure under the large decrease of subgrade reaction due to liquefaction. It is reasonable to consider that the damage at the lower elevation was caused by the permanent ground displacement, since the damage occurred near the boundary between the liquefied and the non-liquefied soil layers.* However, for the damage at the upper

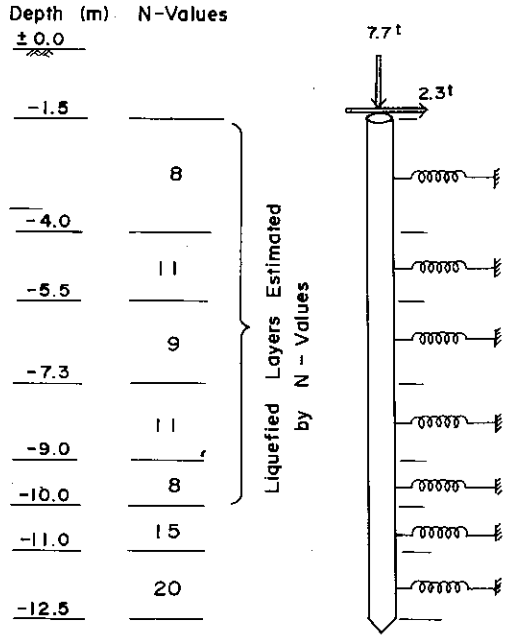

Coefficient of Subgrade Reaction
K-Values (kg/cm³)

DEPTH	CASE-A	CASE-B	CASE-C	CASE-D	CASE-E
±0.0					
	1.0	0.5	0.1	0.05	0.010
-2.5					
	1.4	0.7	0.14	0.07	0.014
-4.0					
	1.1	0.6	0.11	0.06	0.011
-5.8					
	1.4	0.7	0.14	0.07	0.014
-7.5					
-8.5	1.0	0.5	0.10	0.05	0.010
-9.5	1.9	1.9	1.9	1.9	1.9
	2.5	2.5	2.5	2.5	2.5
-11.0					

Fig. 6-1 Numerical model for the analysis of stress in RC piles due to inertia forces

* From the Factor of Liquefaction Resistance, F_L (Appendix III) calculated under an assumption that the maximum acceleration was 159 gal, the soil layer above G.L. −10.0 m was estimated to have been liquefied. (see Fig. 3-12 (c)').

elevation, two causes may be considered: one the inertia forces from the superstructure and the other the permanent ground displacements.

In this section, the stresses in the piles caused by the inertia forces as well as by the permanent ground displacements are analyzed by using numerical models, and the failure process of the piles and the vertical distribution of the permanent ground deformation are also examined.

6.1.1 Stresses in piles caused by inertia forces

The stresses in the piles due to inertia forces were calculated by using the numerical model shown in Figure 6-1. The weight and the horizontal inertia force of the building are assumed to be uniformly borne by all piles, a vertical force of 7.7 tons and a horizontal force of 2.3 tons being applied to the top of each pile.*

Five cases were considered for the coefficient of subgrade reaction. The coefficients of case-A, shown in Figure 6-1, were determined by the procedure specified in the Specification for Highway Bridges Part V, Earthquake Resistant Design in Japan;[13] and were used as the standard values for the case in which no liquefaction occurred in the soil layers. The coefficients of cases B to E were 1/2, 1/10, 1/20, and 1/100 of the standard values, considering the decrease of the soil stiffness due to liquefaction. It was also assumed that the liquefaction occurred in the shallower layers of the ground than GL-10.0 m, based on the calculation of the Factor of Liquefaction Resistance, F_L, as mentioned previously.

The top of the pile was assumed to be connected by a hinge to the concrete base of the building.**

The section of the RC pile is shown in Figure 6-2, and the ultimate bending moment, determined by the compressive failure of the concrete under an axial force of 2.3 tons, is 4.65 ton·m.

Figure 6-3 shows the bending moment of the piles, obtained by the numerical analysis. The bending moment increases as the coefficient of subgrade reaction decreases, and becomes larger than the ultimate strength in cases D and E, where the coefficients are 1/20 and 1/100 of the standard value of non-liquefied layer, respectively. However, in case E, the maximum bending moment occurs 4 to 5 m from the pile top, which is somewhat deeper than the actually observed position of 2.5 to 3.5 m.

From the results of the analysis described above, the following conclusions may be reached. If the

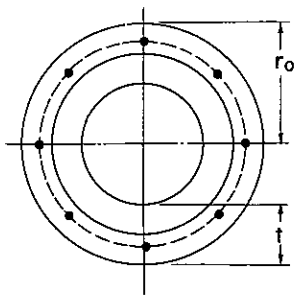

Diameter $2r_o$ = 350 mm
Thickness t = 65 mm
Reinforcement 13 ø x 9

Fig. 6-2 Cross-section of RC pile

* The dead load of the entire three-storey building was assumed to be 1.5 ton/m², and the horizontal force was calculated under the condition that the seismic coefficient was 0.3.

** The tops of the piles are not embedded into the concrete base of the building, nor are the steel reinforcing bars connected, therefore it is considered to be a hinge connection.

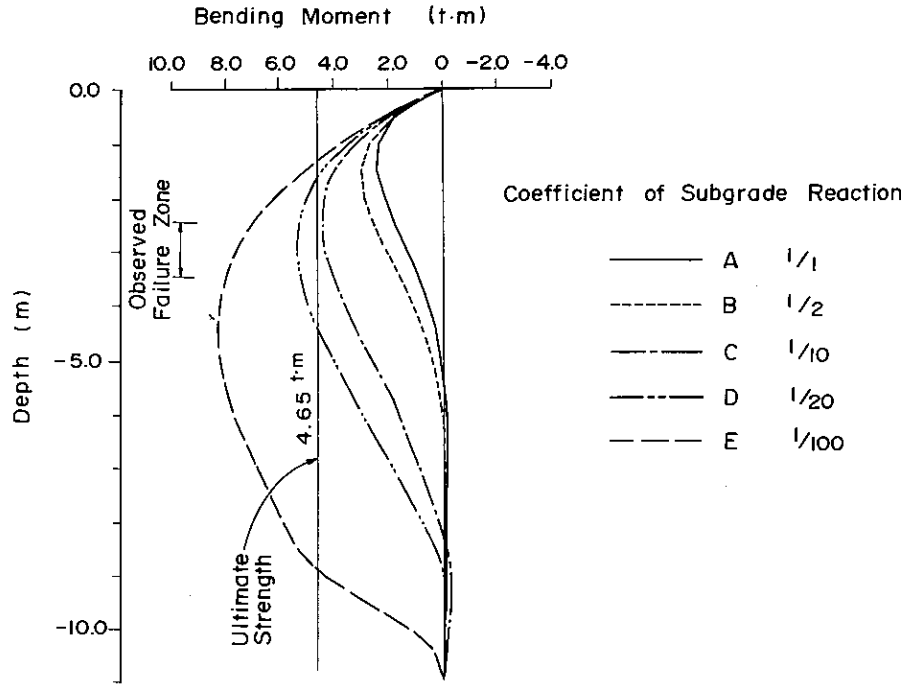

Fig. 6-3 Bending moment of pile due to inertia force

coefficient of subgrade reaction was greatly reduced by liquefaction of the ground, it is possible to consider that the damage at the upper elevation of the piles would have been caused by the inertia force of the superstructure. A comprehensive study of the cause of the damage to the piles is made in 6.1.3.

6.1.2 Stresses in piles caused by the permanent ground displacement

As previously mentioned, it is reasonable to consider that the damage to the piles at the lower elevation was caused by the permanent ground displacements. Therefore, the stress generated in the pile by the permanent ground displacements was analyzed under the following conditions:

(i) Two types of numerical pile models were used, as shown in Figure 6-4. Model II has a plastic hinge at the elevation of −3.0 m. This model assumes that the pile was initially damaged by the inertia force of the building due to the main earthquake motion, and was then subjected to the permanent ground displacement. Model I has no plastic hinge, and assumes that the piles were not damaged by the inertia force.

(ii) Three types of permanent ground displacements were considered, as shown in Figure 6-4. In all cases, the maximum displacement on the ground surface is 1.2 m* and the permanent ground displacement is assumed to have occurred in liquefied soil layers above −10.0 m. Displacement D-1 is case where the permanent ground displacements were distributed in a triangular form, and assumes that the ground deformation occurred uniformly throughout the liquefied layer.

On the other hand displacement D-2 is the case where the permanent ground displacements were distributed in a rectangular form, and assumes that deformation occurred only on the boundary between the liquefied and non-liquefied layers at

* As shown in Fig. 3-10, Kawamura, et al. estimated the displacement of the pile top as 1.0 to 1.2m.

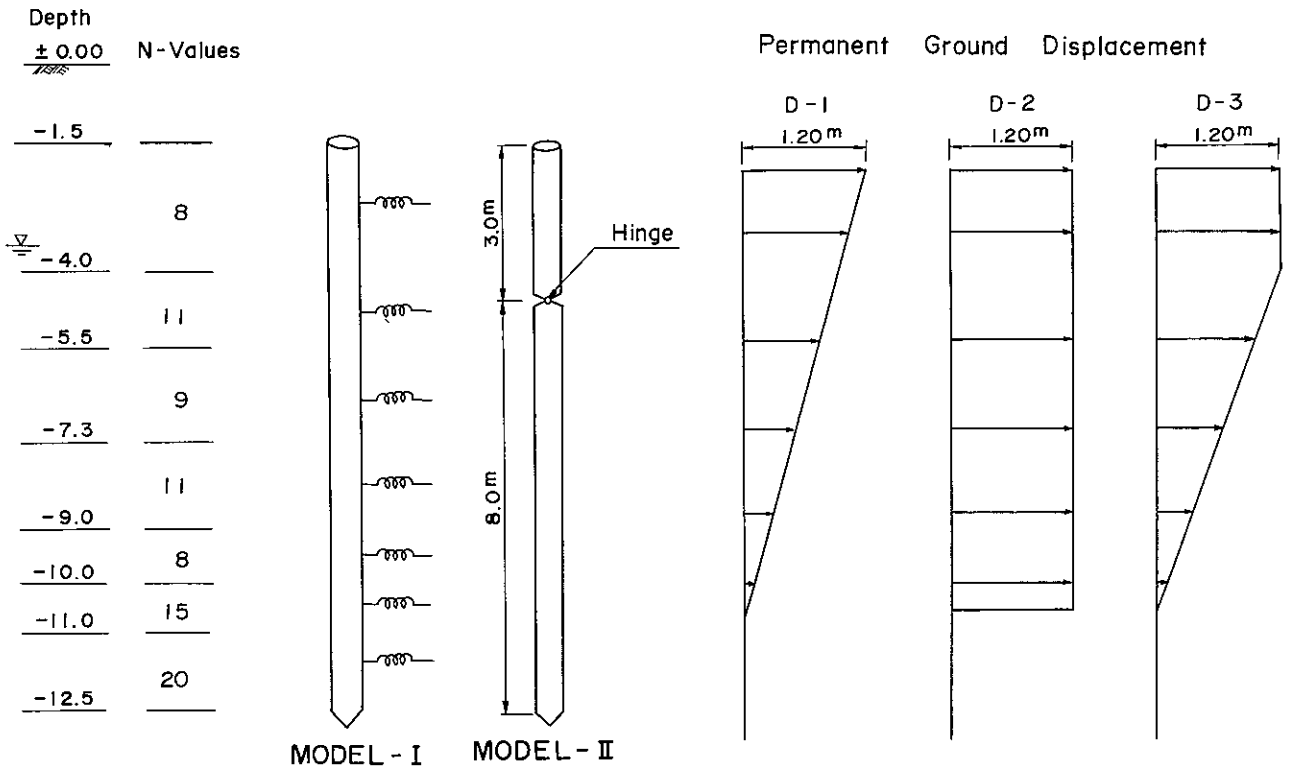

Fig. 6-4 Numerical models from analysis of stress in RC piles due to permanent ground displacements

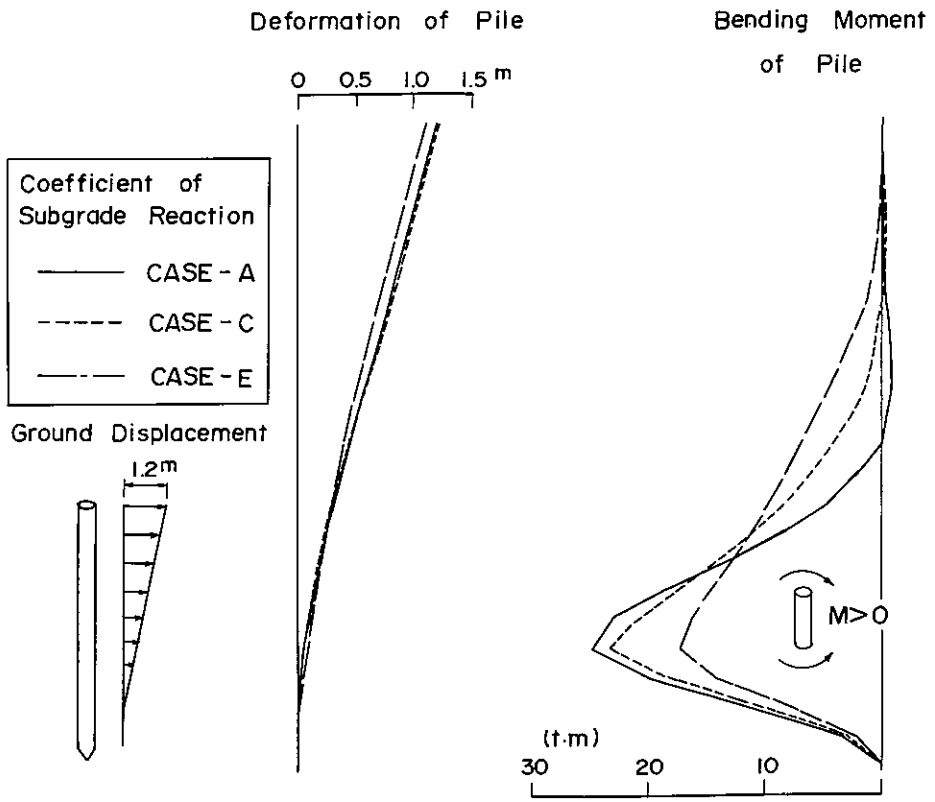

(a) Ground displacement D-1 (Triangular)

Fig. 6-5 Bending moment and deformation of pile (Model I, with no plastic hinge)

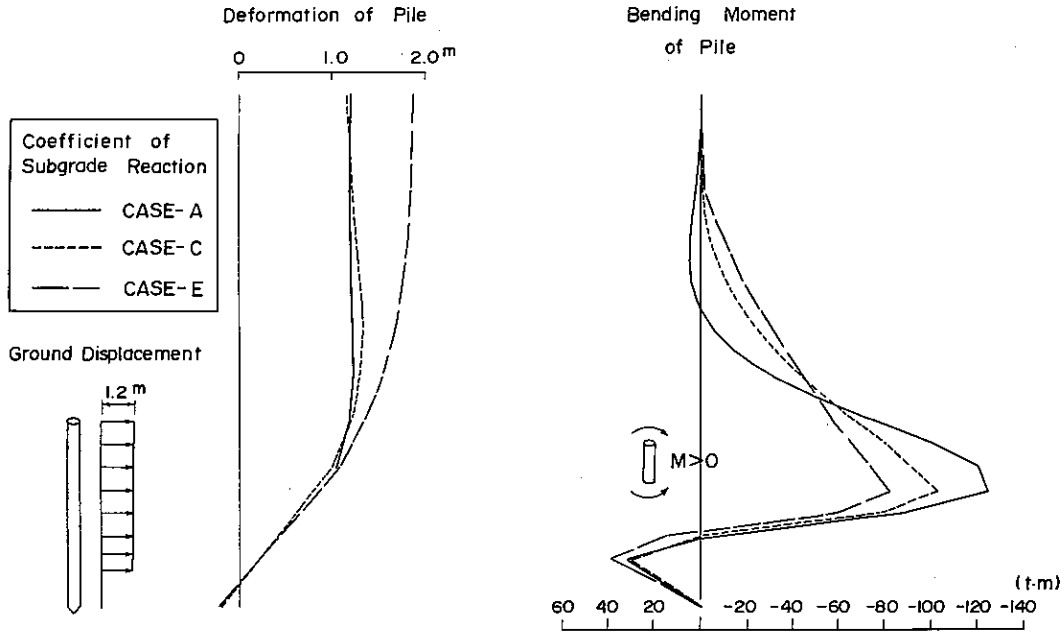

(b) Ground displacement D-2 (Rectangular)

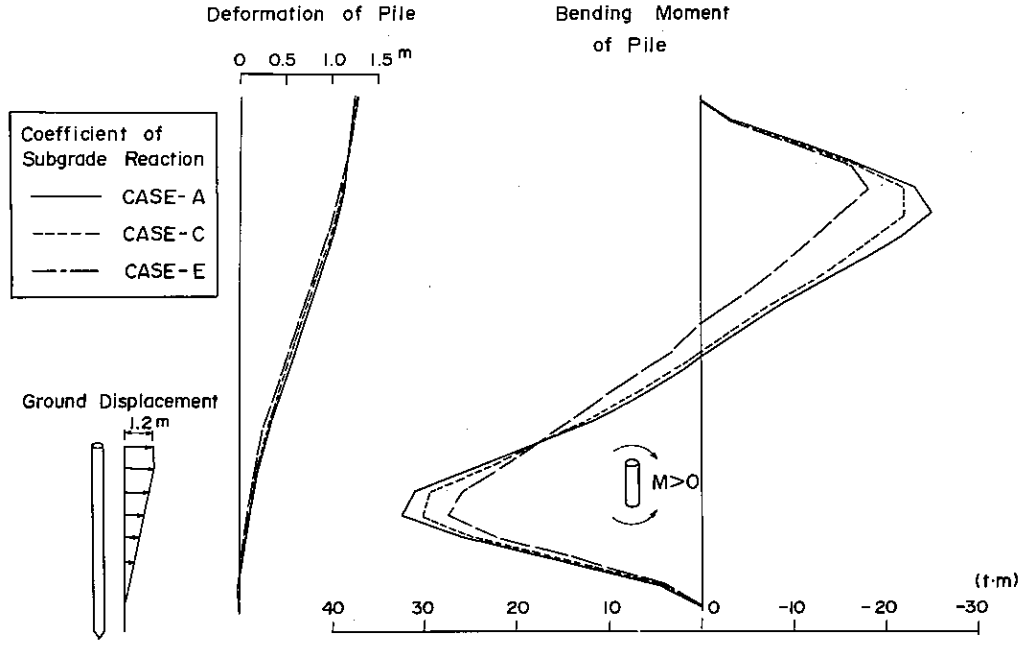

(c) Ground displacement D-3 (Trapezoidal)

Fig. 6-5 Bending moment and deformation of pile (Model I, with no plastic hinge)

the elevation of −10.0 m. Displacement D-3 is the case where they were distributed in a trapezoidal form and assumes that the ground above the groundwater level (−3.5 m) was not liquefied and the ground deformation was linear in the liquefied layer.

(iii) The coefficients of subgrade reaction are the same as the cases shown in Figure 6-1. The coefficients of case-A were determined from the Specification for Highway Bridges Part V, while the coefficients of cases-C and E were 1/10 and 1/100 of those in case-A. In the analysis using the displacement D-3, only the coefficients of the liquefied soil layer between −3.5 and −10.0 m were reduced (cases-C',E').

The bending moment and deformation derived from Model I, with no plastic hinge, are shown in Figure 6-5 while the bending moment of Model II, with a plastic hinge, is shown in Figure 6-6. From the numerical results shown in these figures, the following conclusions are drawn :

(i) In all cases the bending moments caused by ground displacements far exceed the ultimate strength of the pile, 4.65 ton•m

(ii) The bending moments at the lower elevation in the case of displacement D-2 (rectangular shape), shown in Figures 6-5 (b) and 6-6 (b), are negative with respect to the standard rotational direction shown in the figures, while those in the cases of D-1 and D-3 are positive. According to the damage to piles, as shown in Figure 3-10, the damage to the lower elevation of the piles was apparently caused by a positive bending moment, and it can be concluded that the damage to piles at the lower elevation has a high probability to have been caused by permanent ground displacements with either triangular (D-1) or trapezoidal (D-3) distributions. This suggests that the permanent ground displacement was not caused by a sliding on the boundary between the liquefied and the non-liquefied soil layer, but by shearing deformation throughout the liquefied layer.

(iii) As shown in Figure 6-5 (c), the bending

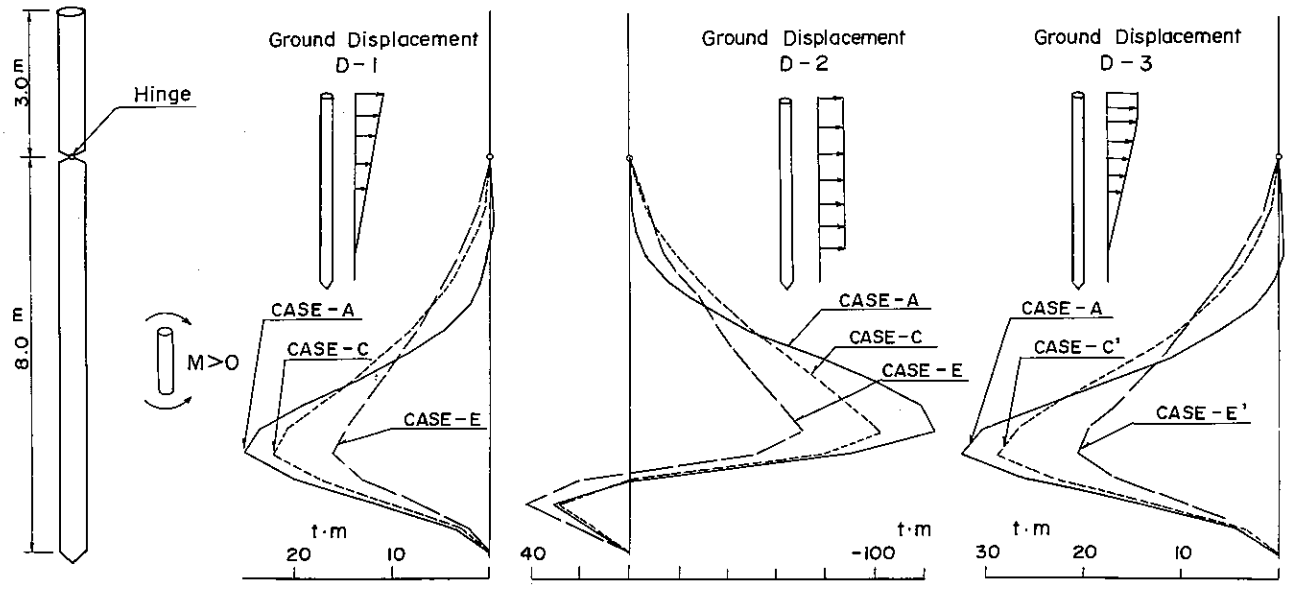

(a) Ground displacement D-1 (b) Ground displacement D-2 (c) Ground displacement D-3

Fig. 6-6 Bending moment of pile (Model II, with plastic hinge)

moment of Model I in the case of displacement D -3, which has a trapezoidal distribution, far exceeds the ultimate strength of the pile at the upper elevation, and its rotational direction is opposite that at the lower elevation. This result would explain the damage to the piles shown in Figure 3-10, and it is highly probable that the damage to the piles at the upper elevation was also caused by the permanent ground displacement.

6.1.3 Consideration of the causes of the damage to the piles

Based on the results of the numerical analyses described in 6.1.1 and 6.1.2, the following conclusions may be drawn as to the causes of the damage to the piles and on the vertical distributions of the horizontal ground displacements.

(i) The damage to the piles at the lower elevation is assumed to have been caused by permanent ground displacements due to soil liquefaction.

(ii) Both the permanent ground displacement and the inertia force of the building are possible causes of the damage at the upper elevation of the piles. However, when taking the following into account it is more rational to assume that the cause is the permanent ground displacement.

As shown in Figure 6-3, the bending moments due to the inertia force barely exceed the ultimate bending moment of piles when the coefficient of subgrade reaction value is reduced to 1/20 of the standard value. On the other hand, when the ground displacement distribution is assumed to be trapezoidal (Figure 6-5 (c), D-3), the bending moment caused at the upper elevation far exceeds the ultimate bending moment. As shown in Figure 3-10 piles were extensively damaged, making it natural to assume that a bending moment far exceeding the ultimate bending moment was applied to the piles. Furthermore, from the damage to the piles, it is apparent that the bending moments at the upper and lower elevations were opposite to each other in rotational direction, which coincides well with the results shown in Figure 6-5 (c).*

(iii) Displacement D-3, which has a trapezoidal distribution, has the highest probability of being the cause of the damage to the piles at both the lower and the upper elevations, since the direction of the bending moment due to displacement D-2 is opposite that of the damage, and the magnitude of bending moment at the upper elevation due to displacement D-1 is smaller than the ultimate strength of the piles, as shown in Figure 6-5.

Trapezoidal distribution D-3 is the case in which it was assumed that the soil layer below the water level, G.L. −3.5 m and above G.L. −10.0 m had been liquefied and that a linear shearing deformation occurred in the liquefied layer.

The assumption above mentioned can explain the result discussed in Section 4.1 that the magnitude of permanent ground displacement depends on the thickness of liquefied layer.

---

* Assuming that the upper parts of the piles were damaged by the inertia forces, the directions of the bending moments at the upper and lower elevations are not necessarily opposite in direction.

6 . 2 Numerical analysis of buried steel gas pipe damaged by the 1983 Nihonkai-Chubu earthquake

The permanent ground displacements and the damage to buried gas and water pipes during the 1983 Nihonkai-Chubu earthquake were described in Section 2.2. Also, in Chapter 5, it was established that the damage rate for large size gas pipes has a relatively high correlation with the permanent ground displacements and the permanent ground strains.

In this section, the failure process of welded steel gas pipes with a diameter of 80 mm is discussed by numerical analyses, based on the permanent ground displacements.

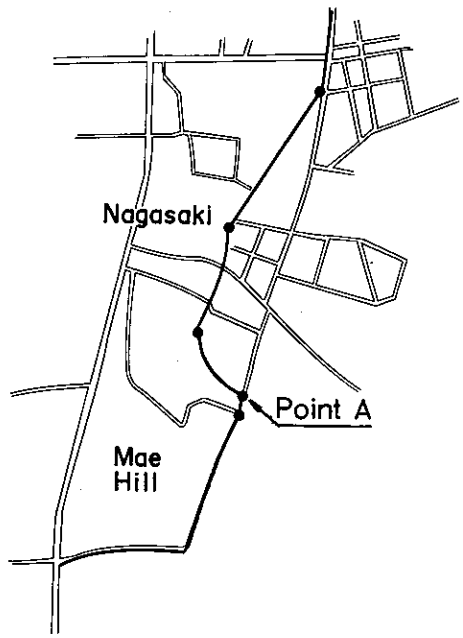

Fig. 6-7 Locations of damage to welded steel gas pipes in Noshiro City (in southern area, see Figure 2-8)

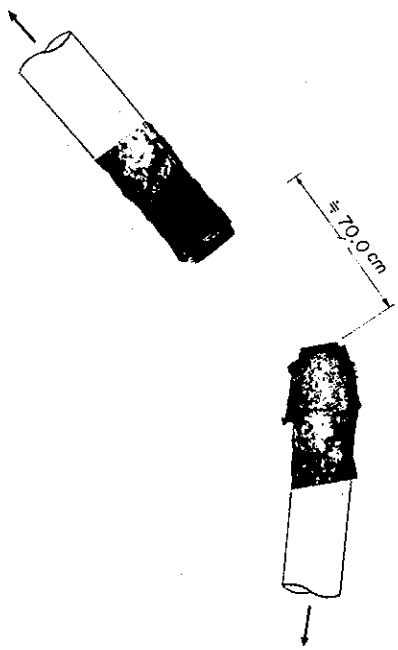

Photo 6-1 Damage to welded steel gas pipe to point A

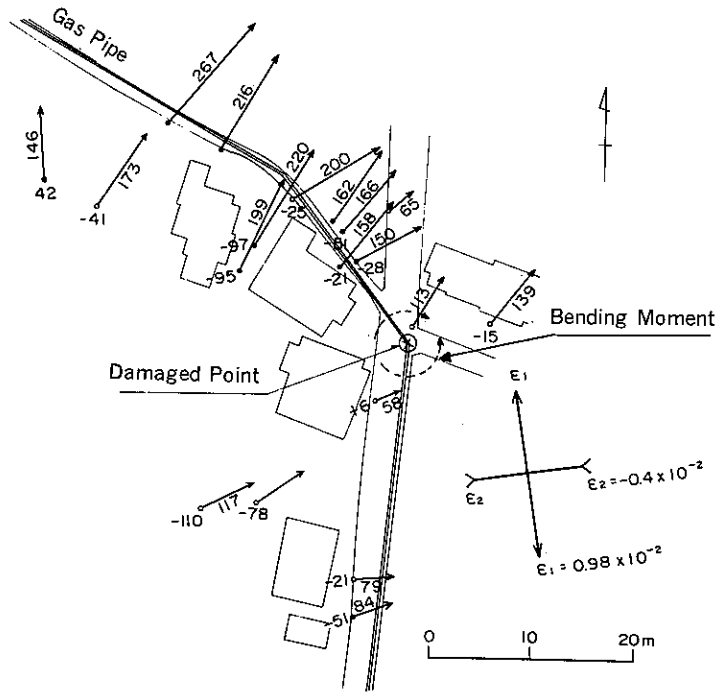

Fig. 6-8 Permanent ground displacement measured in vicinity of Point A (m)

6.2.1 Damage to welded steel gas pipes and the permanent ground displacements measured in the vicinity

In the southern area of Noshiro City, welded steel gas pipes with a diameter of 80 mm were damaged at five locations, as shown in Figure 6-7. In this section, the damage at the location A in the figure, is studied by numerical analysis. This location is near the toe of the slope of Mae Hill, on the slope of which the permanent ground displacement exceeded 5 m, and the occurrence of liquefaction was confirmed by the observation of many sand volcanoes and cracks on the ground surface.

Photo 6-1 shows the damaged pipe at point A,[14] while Figure 6-8 shows the permanent horizontal ground displacements in the vicinity measured by the aerial photograph survey.

The pipe was broken at the welded joint of a 45 degree elbow and it was discovered upon excavation that the two broken ends were separated from each other by about 70 cm, as shown in Photo 6-1. From the examination of the broken ends of the pipe, it was shown that a large bending moment at the elbow, caused by a tensile force in the straight portion of the pipe, was the direct cause of the breakage. The permanent ground displacements in this neighborhood reach 2.0 m and are mostly perpendicular to the pipe axis. The ground displacements seemed to cause a bending moment, enlarging the angle of the bend, as shown in Figure 6-8. The maximum principal strain calculated from permanent ground displacements was tensile of about 1.0%, as shown in the figure.

6.2.2 Numerical analysis of the deformation of the welded steel gas pipe

The deformation and stress of the above-mentioned damaged gas pipe was analyzed by using a numerical method, the "response displacement method",* and the causal relationship between the damages and the permanent ground displacements was discussed. The conditions of numerical analysis were as follows:

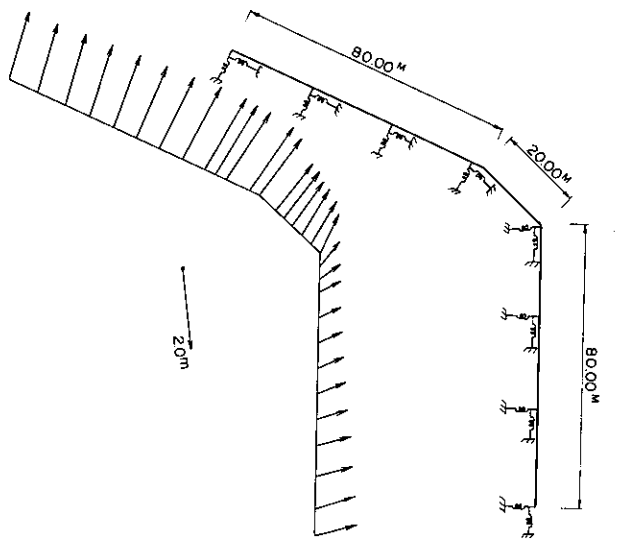

Fig. 6-9 Numerical model for stress analysis of buried pipe

Table 6-1 Coefficient of subgrade reaction and friction strength between pipe and ground

CASE	Coefficeient of Subgrade Reaction	Friction Strength
A−1	0.05 kg/cm³	0.1 kg/cm²
A−2	0.05 〃	0.05 〃
A−3	0.05 〃	0.01 〃

* Response Displacement Method: in this method the deformation and the stresses of the buried pipes are calculated by using a beam model on elasto-plastic foundation, where the ground displacement is statically applied to the beam model.

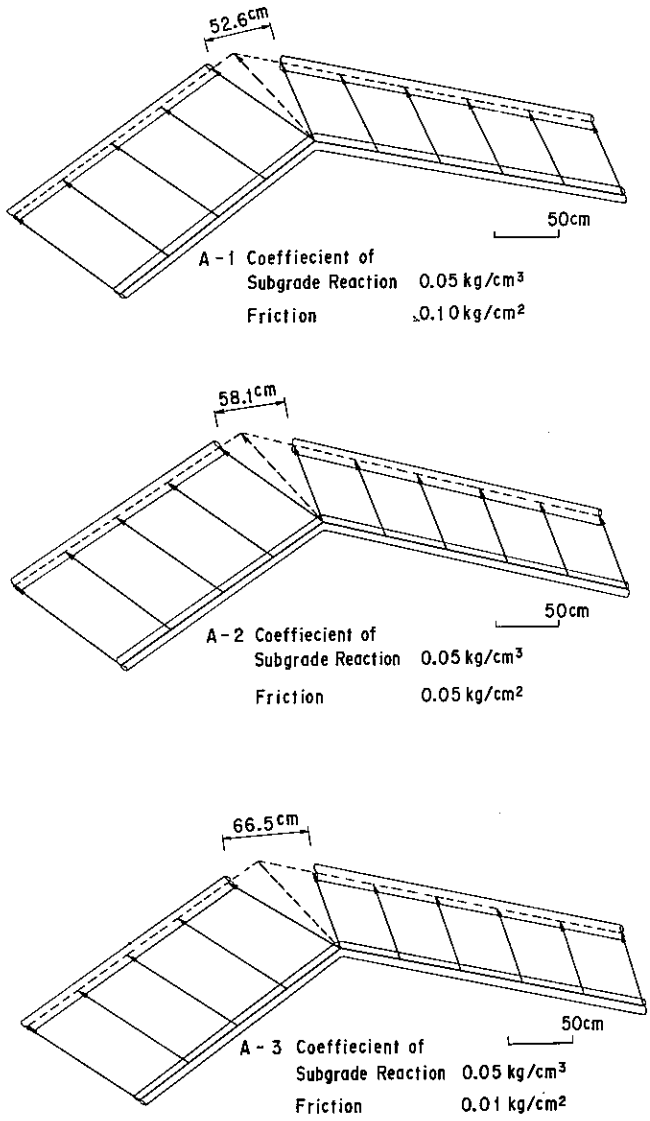

Fig. 6-10 Displacement of pipe

(i) The input ground displacement is determined by linear interpolation of the measured ground displacements, as shown in Figure 6-9.

(ii) The coefficient of subgrade reaction and the friction strength between the buried pipes and the ground were assumed to be as shown in Table 6-1.*

(iii) The pipe is assumed to be elastic, but the welded joint at the bend would be broken and separated when the bending tensile stress at the joint exceeds 4000 kg/cm².**

Figure 6-10 shows the calculated displacement of the gas pipe. The dotted line in the figure indicates the vector of the input displacement used for analysis, and the solid line the direction of movement of the pipe. In all cases shown in the figure, slippage occurred between pipes and the ground after the breakage, and the broken two ends had become separated. As the friction strength between the pipe and the ground decreases, the slippage increase and so does the separation between the breaks.

As previously mentioned, the measured separation of the broken ends was about 70 cm, and the results of analysis by case A-3, where the friction strength between the pipe and the ground was assumed to be 0.01 kg/cm² (1/10 of the standard value of the Design Practice), agrees well with the actually measured values.

From the numerical results above mentioned it is concluded that the damage process of the gas pipe can be pursued by considering the permanent ground displacements measured in the surrounding area.

---

* The Design Practice of Earthquake Resistance of Buried Gas Pipelines[15] determines the standard values of the coefficient of subgrade reaction and friction strength in the case of non-liquefaction as being about 0.6 kg/cm/cm² and 0.1~0.3 kg/cm², respectively. In this analysis, by considering a large decrease in the soil stiffness and effective stress due to liquefaction, much smaller values, as shown in the table, were also used. The same value of the coefficient was used for both the axial and the lateral directions.

** The damage was the breakage of welded joint at a bend. Although it is difficult to estimate the strengths of the welded joint, it was tentatively assumed to be 4,000 kg/cm² in this analysis. However, it was confirmed that the effect of this value on the deformation and the stress of pipes after the breakage was minimal.